Preprints of the 23rd IFAC World Congress
Busan, Republic of Korea, August 23-28, 2026

Safe Multi-Agent UAV-UGV Rendezvous in Dynamic Environments

Ghewa Masry * **David Vieira** * **Rodolfo Orjuela** *
Thomas Meurer ** **Michel Basset** *

* *Institut de Recherche en Informatique, Mathématiques, Automatique et Signal (IRIMAS UR 7499), Université de Haute-Alsace, 68093 Mulhouse, France (e-mail: {ghewa.masry, david.vieira-gois-fernandes, rodolfo.orjuela, michel.basset}@uha.fr.*
** *Karlsruhe Institute of Technology (KIT), 76131 Karlsruhe, Germany (e-mail: thomas.meurer@kit.edu)*

Abstract: Multi-agent systems (MAS) offer significant advantages that can enhance performance across various domains. However, a critical challenge is to guarantee the agents' safety while navigating environments with both static and dynamic obstacles. This paper presents a distributed model predictive control (MPC) framework to coordinate multiple unmanned aerial vehicles (UAVs) and unmanned ground vehicles (UGVs) to rendezvous at predefined locations while simultaneously avoiding collisions with obstacles and other agents. An obstacle aggregation strategy is adopted to reduce computational complexity and enhance scalability. Simulation results demonstrate the effectiveness of the proposed approach to safely rendezvous in a dynamic environment.

Keywords: Multi-vehicle systems, navigation and control for AVs, collision avoidance, model predictive control, distributed control.

1. INTRODUCTION

Coordinated multi-agent systems (MAS) have gained significant research attention in recent years, finding application in various domains such as search and rescue, manufacturing, surveillance, environmental monitoring and exploration. A main area of interest is the cooperation between unmanned aerial vehicles (UAVs) and unmanned ground vehicles (UGVs), which leverages their complementary capabilities to efficiently complete complex tasks (Chai et al. (2024); Munasinghe et al. (2024)). An interesting application of aerial-ground cooperation is that the UGV can serve as a mobile recharging station for the UAV, which addresses the flight time limitation of UAVs (Asghar et al., 2023). This requires the coordination between the two vehicles to rendezvous at a location where the UAV can safely land on the UGV for recharging. However, while navigating the environment, each of the vehicles may encounter static or dynamic obstacles as well as other agents. Therefore, collision avoidance is crucial to guarantee the safety of the agents (Oh et al., 2025).

Various approaches have been proposed in the literature to address the aerial-ground rendezvous and autonomous landing problem of a UAV on a UGV, yet only few address collision avoidance in this context. Considering UGV obstacle avoidance, Bacheti et al. (2021) present a path-following formation controller based on the virtual structure to guide the UAV-UGV formation, considering that the UAV should land on the UGV but neither aerial nor moving obstacles are considered. For UAV obstacle avoidance, authors in Guo et al. (2022) present a vision-based planner where the UAV detects the UGV, and a B-spline curve and A^* algorithm strategy generates the collision-free trajectory for the UAV. In a previous work Masry et al. (2025), the simultaneous obstacle avoidance of both the UAV and UGV is considered. A distributed consensus-based approach incorporating the virtual force obstacle avoidance method is presented to safely guide the vehicles to rendezvous.

While in the previously mentioned works only one UAV and one UGV are considered, Sankaranarayanan et al. (2024) consider the landing of multiple UAVs and thus the inter-agent collision avoidance between them. A spherical control barrier function (SCBF) is employed in a centralized architecture for collision avoidance along with a landing CBF for safe landing. However, neither static nor dynamic obstacles are considered, and collision avoidance for the ground vehicles is also not addressed. While this can be extended by including more CBFs, doing so would increase the computational complexity.

In this work, the rendezvous problem of multiple UAVs and UGVs is addressed, incorporating both ground and aerial collision avoidance in dynamic environments. A distributed model predictive control (MPC) approach is employed to plan the trajectories and generate the control inputs for each agent while taking into account dynamic constraints and avoiding obstacles. Since the environment

⋆ This work is supported by the collaboration between IRIMAS-UHA (France) and KIT (Germany) in the framework of the Digital Process Engineering for Sustainable Materials and Energy. This work was funded by the European Interreg Rhin-Superieur program through the RobotHub Academie and RobotHub Transfer projects.

©2026 the authors. Accepted by IFAC for publication under a Creative Commons Licence CC-BY-NC-ND

contains both static and dynamic obstacles, including other agents, the number of constraints in the MPC problem would increase drastically with the number of obstacles, increasing computational complexity. Therefore, as presented in Yu et al. (2025), an obstacle aggregation strategy is adopted where the multiple obstacle constraints can be aggregated into a single one. However, in scenarios where multiple obstacles block the ground vehicle's path, the MPC alone would require a very long prediction horizon to be able to find a feasible trajectory, which is computationally expensive. Consequently, a global path considering the static obstacles is first generated using the A^* algorithm, which the MPC then follows while locally avoiding dynamic obstacles and other agents. Moreover, to guarantee recursive feasibility, a safe backup trajectory is generated at all times, requiring the vehicle to stop (UGV) or hover (UAV) at the end of its prediction horizon, similarly to Rubinacci et al. (2025). While the vehicle does not actually stop due to MPC replanning, this ensures a safe and feasible backup plan at all times. Thus, the contributions of this work can be combined as follows:

- A distributed MPC formulation to coordinate between multiple UAVs and UGVs to safely rendezvous in an environment with static and dynamic obstacles.
- An obstacle aggregation strategy adopted to enhance scalability and reduce computational complexity.
- A recursive feasibility guarantee for UAVs and UGVs ensuring safety.

The rest of the paper is organized as follows: Section 2 briefly presents the vehicle models. Section 3 presents the proposed MPC approach to generate the safe trajectories for each vehicle. Simulation results are presented in Section 4. Finally, the conclusion and future perspectives are given in Section 5.

2. SYSTEM MODELING

The ground and aerial vehicles' models and their feedback linearization controllers are adopted from Daly et al. (2015) due to their simplicity while still adequately accounting for the agents' dynamics. The reader is referred to Daly et al. (2015) for more details.

2.1 UAV model

The considered aerial vehicle is a quadrotor whose dynamic model has the following state vector (Daly et al., 2015):

$$P_a = [x_a, \dot{x}_a, y_a, \dot{y}_a, z_a, \dot{z}_a, \phi_a, \dot{\phi}_a, \theta_a, \dot{\theta}_a, \psi_a, \dot{\psi}_a]^T, \quad (1)$$

where $p_a = [x_a, y_a, z_a]^T$ is the position vector of the aerial vehicle, $v_a = [\dot{x}_a, \dot{y}_a, \dot{z}_a]^T$ the velocities, $[\phi_a, \theta_a, \psi_a]$ the Euler angles and $[\dot{\phi}_a, \dot{\theta}_a, \dot{\psi}_a]$ the angular velocities.

The gravity g and the total thrust U_1 are considered to be the only external forces acting on the quadrotor. The altitude is then feedback linearized into

$$\ddot{z}_a = u_z, \quad (2)$$

and the quadrotor's positions can be treated as a linear double integrator

$$\begin{bmatrix} \ddot{x}_a \\ \ddot{y}_a \end{bmatrix} = u_a = \begin{bmatrix} u_{a,1} \\ u_{a,2} \end{bmatrix} \quad (3)$$

with the virtual inputs u_a, where

$$\begin{bmatrix} \theta_a \\ \phi_a \end{bmatrix} = \frac{m}{U_1} \begin{bmatrix} \cos\psi_a & \sin\psi_a \\ \sin\psi_a & -\cos\psi_a \end{bmatrix} u_a. \quad (4)$$

Herein, m is the mass and an inner PD controller is used for the attitude control to track the desired generated values of θ_a and ϕ_a, as proposed in Daly et al. (2015).

2.2 UGV model

The kinematic model of a skid-steered ground vehicle is used from Daly et al. (2015); Kozłowski and Pazderski (2004):

$$\begin{bmatrix} \dot{x}_g \\ \dot{y}_g \\ \dot{\psi}_g \end{bmatrix} = \begin{bmatrix} \cos\psi_g & x_{ICR}\sin\psi_g \\ \sin\psi_g & -x_{ICR}\cos\psi_g \\ 0 & 1 \end{bmatrix} \begin{bmatrix} v_x \\ w \end{bmatrix}, \quad (5)$$

where $p_g = [x_g, y_g]^T$ is the position vector of the ground vehicle, ψ_g is the angle of the body-fixed frame in the global coordinates, and x_{ICR} represents the x projection of the instantaneous center of rotation (ICR) of the vehicle into the body-fixed frame for which a constant approximation x_0 is used. Moreover, v_x and w denote the x-component of the translatory and the angular velocity, respectively.

The feedback linearization controller using input-output feedback linearization is then presented by (Daly et al., 2015):

$$\begin{bmatrix} v_x \\ w \end{bmatrix} = \begin{bmatrix} \cos\psi_g & \sin\psi_g \\ \frac{\sin\psi_g}{x_0} & -\frac{\cos\psi_g}{x_0} \end{bmatrix} \begin{bmatrix} u_{g,1} \\ u_{g,2} \end{bmatrix}. \quad (6)$$

As a result, the ground vehicle's position can be treated as a linear single integrator:

$$\begin{bmatrix} \dot{x}_g \\ \dot{y}_g \end{bmatrix} = u_g = \begin{bmatrix} u_{g,1} \\ u_{g,2} \end{bmatrix}, \quad (7)$$

where $u_{g,1}$ and $u_{g,2}$ denote the virtual control inputs for the x and y positions of the UGV, respectively.

3. DISTRIBUTED MPC FRAMEWORK

A distributed MPC approach is proposed to address the multi UAV-UGV rendezvous problem, where each vehicle generates its own trajectory over a prediction horizon while respecting dynamic and safety constraints. The following assumptions are considered:

- Only the UGV is aware of the rendezvous location, therefore each UAV-UGV pair share their position information to move towards each other.
- Agents of the same type share their planned trajectories to guarantee inter-agent collision avoidance. Here, it is assumed that there is no communication loss or delay between the communicating agents since this is not the focus of this paper.
- Obstacle positions are available in real-time. Each obstacle has a position $p_o^i(t) = [x_o^i(t), y_o^i(t), z_o^i(t)]^T$ and a radius r_o^i that includes the obstacle's radius as well as the radius of the smallest circle encompassing the agent in addition to a safety margin. For static obstacles, p_o^i is fixed over time.

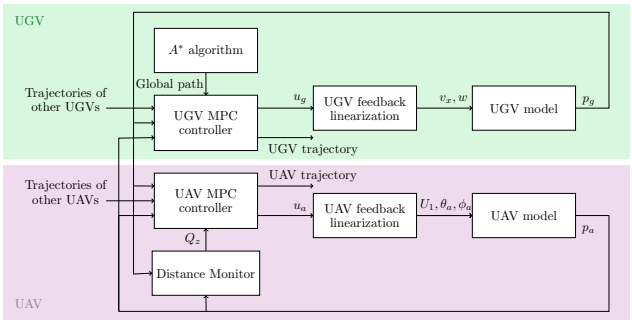


Fig. 1. MPC planner architecture for each UAV-UGV pair.

The architecture for each UAV-UGV pair is presented in Fig. 1. Each UGV receives its reference path, which is generated by the A^* algorithm, the position of its corresponding UAV, as well as the trajectories of the other UGVs. The local MPC controller then tracks the global path and penalizes the horizontal distance towards the UAV while avoiding dynamic obstacles. In parallel, each UAV receives the position of its corresponding UGV and the trajectories of the other UAVs, the MPC controller then penalizes the distance towards the UGV while avoiding obstacles. Moreover, the distance between each UAV and its corresponding UGV is monitored so that the UAV can safely start its landing maneuver when the pair is at a sufficiently close distance. These controllers are described in detail in the subsequent sections.

3.1 UGV planning and control

For each ground vehicle, initially a global path is generated using the A^* algorithm taking into consideration the static obstacles in the environment. Then, the MPC-based local planner and controller generates the optimal control inputs to track this reference while avoiding dynamic obstacles, including other agents, and respecting constraints.

The MPC problem reads:

$$\begin{aligned} J_g = &\int_{t_0}^{t_1} (Q_{ref}||p_{ref} - p_g||^2 + Q_{ga}||p_{a_{x,y}} - p_g||^2)dt \\ &+ \int_{t_0}^{t_1} u_g^T R_g u_g dt + w_o J_o + J_{bu_g}, \end{aligned} \tag{8}$$

subject to

$$\dot{p}_g = f(p_g, u_g) \tag{9a}$$
$$u_{g_{\min}} \leq u_g \leq u_{g_{\max}} \tag{9b}$$
$$\mathcal{G}(p) \leq 0 \tag{9c}$$
$$p_g(t_f) \in P_{gt}. \tag{9d}$$

In (8), the first term minimizes the error to the global path, while the second term is to encourage the ground vehicle to move towards the aerial vehicle, and the third term minimizes the control effort. The diagonal weight matrices Q_{ref} , Q_{ga}, and R_g penalize the corresponding terms. These terms result in the primary trajectory over the duration $t_0 - t_1$, while J_{bu_g}, given in (12), generates the backup trajectory guiding the UGV to safety over the duration $t_1 - t_f$.

The term J_o with weight w_o represents the obstacle avoidance soft constraint, which increases the cost function when the UGV is close to the obstacles as given in Yu et al. (2025), i.e.,

$$J_o = \int_{t_0}^{t_f} (\tanh(a_t k_o(t) + 1))dt, \tag{10}$$

where a_t represents the size of the penalized area and $k_o(t)$ is given by

$$\begin{aligned} k_o^i(t) = &\left(\frac{x_g(t) - x_o^i(t)}{r_o^i}\right)^2 + \left(\frac{y_g(t) - y_o^i(t)}{r_o^i}\right)^2 \\ &+ \left(\frac{z_g - z_o^i(t)}{r_o^i}\right)^2. \end{aligned} \tag{11}$$

Noting that for the UGV, the z-component is considered to be fixed at $z_g = 0$.

Finally, J_{bu} is the backup trajectory term that aims to minimize the length of the trajectory that guides the UGV to the terminal safe stop with a weight w_{bu}. This is given by

$$J_{bu_g} = \int_{t_1}^{t_f} w_{bu}||\dot{p}_g(t)||dt. \tag{12}$$

The cost function in (8) is subject to a set of hard constraints presented in (9), where (9a) and (9b) represent the vehicle dynamic model, here the single integrator in (7) discretized using zero-order hold discretization with sampling time T_s, and the bounds on the control inputs, respectively.

With the purpose of reducing computational complexity, the multiple constraints needed to handle each obstacle separately are instead aggregated into a single one. Eqn. (9c) is the aggregated obstacles' hard constraint that guarantees obstacle avoidance, noting that the soft constraint J_o encourages obstacle avoidance but it is unable to guarantee it on its own. As presented in Yu et al. (2025), the function reads

$$\mathcal{G}(p) = \sum_{i=1}^{n_o} \sum_{j=1}^{n_{ds}} e^{-\rho d_o^i(\mathcal{T}(j))} - 1 \leq 0 \quad \forall \rho > 0, \tag{13}$$

with

$$\begin{aligned} d_o^i = &\left(x_g(t) - x_o^i(t)\right)^2 + \left(y_g(t) - y_o^i(t)\right)^2 \\ &+ \left(z_g - z_o^i(t)\right)^2 - (r_o^i)^2, \end{aligned} \tag{14}$$

where n_o is the number of obstacles, n_{ds} is the number of discretized states along the trajectory and d_o^i the distance from the vehicle to the obstacle. Herein, $\mathcal{T}(j)$ represents the mapping from the j^{th} discretized point on the trajectory to time t. The parameter ρ represents the curvature parameter of the constraint aggregation and it controls the conservativeness. Taking a high value of ρ reduces the unsafe region to the original obstacles so that

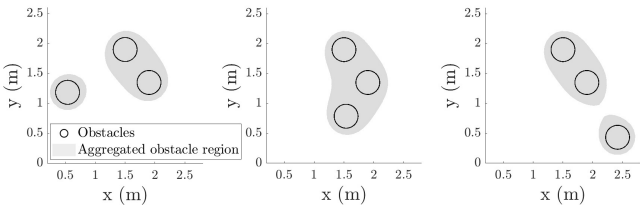


Fig. 2. Aggregation of a dynamic obstacle with $\rho = 4$.

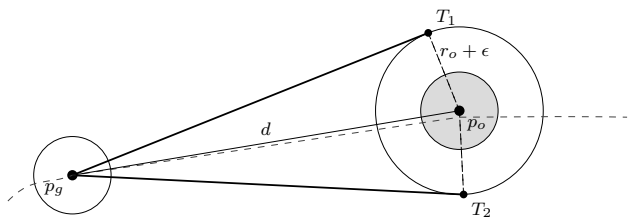


Fig. 3. Tangent points as virtual goal candidates.

narrow passages can be allowed while a smaller ρ results in a more conservative unsafe region marking them unsafe. The aggregated region is also able to expand to include dynamic obstacles when they are sufficiently close, this is demonstrated in Fig. 2. Other agents share their planned trajectories over the horizon and so a safe plan is generated by anticipating any collisions.

Finally, the terminal constraint in (9d) guarantees recursive feasibility by forcing the UGV to stop at the end of the horizon at a point in the safe set $P_{gt} = \{p_g \in \mathbb{R}^2 : \mathcal{G}(p) \leq 0, \dot{p}_g = 0\}$.

If a dynamic obstacle blocks the path, the MPC switches off the reference tracking cost ($Q_{ref} = 0$) and a virtual goal is set as one of the tangent points on the circle with radius $r_o + \epsilon$ as seen in Fig. 3. The safety of the tangent points is first evaluated. If both points lie outside the aggregated obstacles' region, the tangent point that is closest to the next safe point on the global path is selected as the virtual goal. This allows the agent, if possible, to go around the obstacle and back to the safe part of the reference path. It is noteworthy that in the worst case the MPC falls back to a safe stop if no feasible path is found.

3.2 UAV planning and control

For each UAV a MPC-based controller generates the safe trajectory and the optimal control inputs to meet the corresponding UGV while avoiding collisions. The MPC formulation has the following cost function

$$J_a = \int_{t_0}^{t_1} (Q_{ag}||p_g - p_{a_{x,y}}||^2 + Q_{as}||v_a||^2 + Q_z||z_l - p_{a_z}||^2)dt + u_a^T R_a u_a + w_o J_o + J_{bu_a}, \tag{15}$$

subject to

$$\dot{p}_a = f(p_a, u_a) \tag{16a}$$
$$u_{a_{\min}} \leq u_a \leq u_{a_{\max}} \tag{16b}$$
$$\mathcal{G}(p) \leq 0 \tag{16c}$$
$$p_a(t_f) \in P_{at}. \tag{16d}$$

Here, the first term in (15) minimizes the error towards the UGV while the second one aims to drive the velocity towards zero and improve smoothness. The diagonal weight matrices Q_{ag} , Q_{as}, and R_a penalize the corresponding terms. The third term controls the aerial vehicle's altitude. When the UAV is at a sufficiently close horizontal distance from the ground vehicle, altitude control is activated so that the UAV descends gradually according to the weight Q_z given by

$$Q_z = \frac{1}{1 + e^{-s(d_l - ||p_g - p_{a_{x,y}}||)}}, \tag{17}$$

where s controls the steepness of the sigmoid function and d_l is the distance threshold at which the landing is activated.

The term J_o corresponds to (10) with $p_a = [x_a, y_a, z_a]^T$. Meanwhile, the term to minimize the backup trajectory for a double integrator is here given by

$$J_{bu_a} = \int_{t_1}^{t_f} w_{bu}||\dot{p}_g(t)||^2 dt. \tag{18}$$

The constraints in (16) present the discretized vehicle model, here the double integrator model from (2) and (3), the control input bounds, and the aggregated obstacles' constraint as given in (16a), (16b), and (16c), respectively. Finally, the terminal constraint (16d) guarantee recursive feasibility by forcing the UAV to hover at the end of the horizon at a point in the safe set $P_{at} = \{p_a \in \mathbb{R}^3 : \mathcal{G}(p) \leq 0, \dot{p}_g = 0, \ddot{p}_g = 0\}$.

4. SIMULATION RESULTS

The distributed MPC controllers are validated on MATLAB/Simulink using the CasADi framework (Andersson et al., 2019). Three pairs of aerial and ground vehicles are considered, where each UAV with p_{a_i} needs to rendezvous with its corresponding UGV p_{g_i}. The initial conditions for the ground and aerial vehicle pairs are $p_{g_{10}} = [0, 3]^T$, $p_{g_{20}} = [0, 1]^T$, $p_{g_{30}} = [0, -1]^T$, $p_{a_{10}} = [6, 6, 6]^T$, $p_{a_{20}} = [5, 4, 5]^T$, $p_{a_{30}} = [5, 7, 4]^T$ respectively.

The desired rendezvous points are set as $p_{r_1} = [5, 0, 0]^T$, $p_{r_2} = [5, 2, 0]^T$, and $p_{r_3} = [5, 4, 0]^T$. Noting that the aerial vehicle is considered to land at $z_l = 0.5$ m.

4.1 Scenario 1

The parameters of the controllers are as follows: $T_s = 0.02$, $Q_{ref} = 2\,\mathbf{I}_2$, $Q_{ga} = 0.1\,\mathbf{I}_2$, $R_g = 1.5\,\mathbf{I}_2$, $w_o = 5$, $w_{bu} = 2$, $Q_{ag} = 1.2\,\mathbf{I}_2$, $Q_{as} = 0.5\,\mathbf{I}_3$, $R_a = 0.5\,\mathbf{I}_3$, $a_t = -1$, $d_l = 0.8$ m, and $s = 3$. Herein, $\mathbf{I}_2 \in R^{2\times 2}$ and $\mathbf{I}_3 \in R^{3\times 3}$ denote the identity matrices.

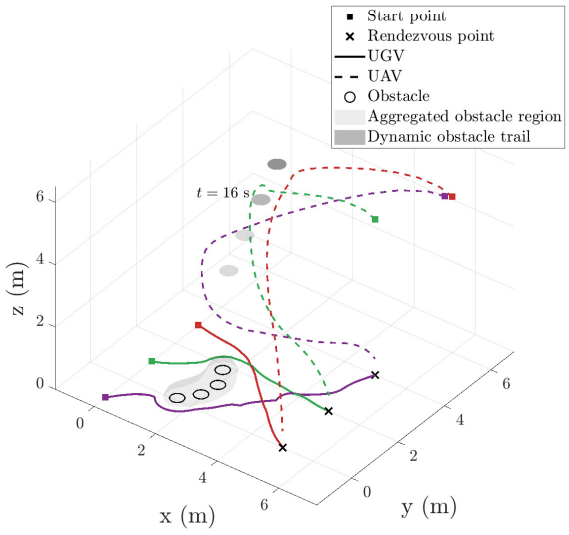


Fig. 4. Trajectories of UGVs and UAVs.

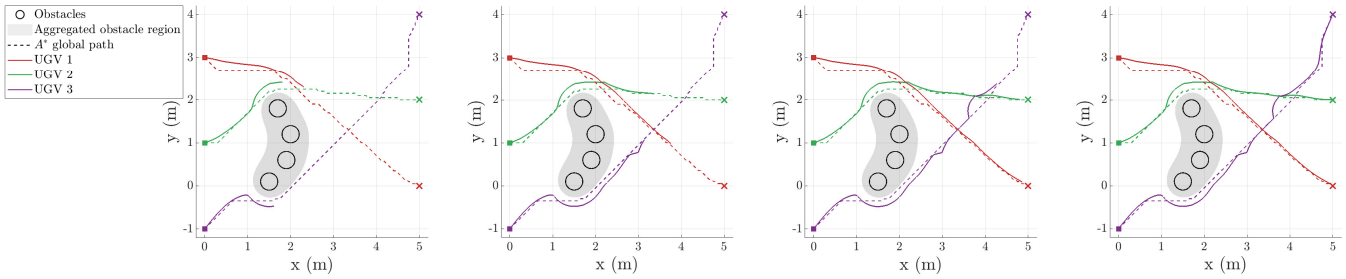


Fig. 5. Trajectories followed by UGVs at different time steps.

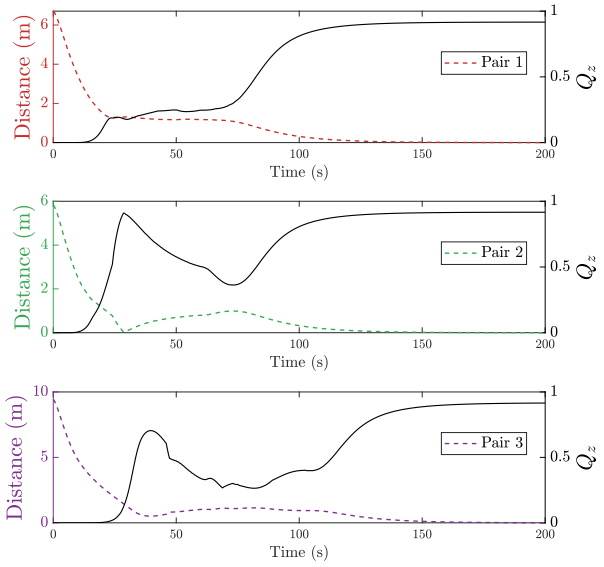


Fig. 6. Variation of Q_z according to the horizontal distance between each pair of vehicles.

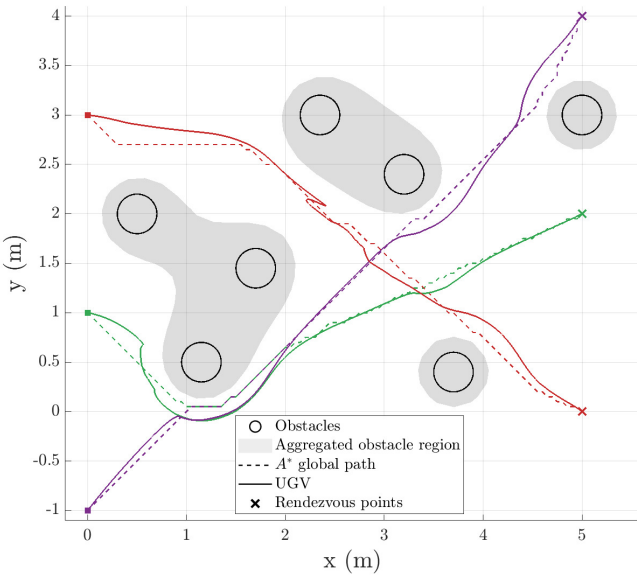


Fig. 7. Trajectories followed by UGV with $\rho = 2$.

In the first scenario, the controllers are tested with a set of obstacles fixed at the following positions $p_{o_1} = [1.5, 0.1, 0]^T, p_{o_2} = [1.9, 0.6, 0]^T, p_{o_3} = [2, 1.2, 0]^T, p_{o_4} = [1.7, 1.8, 0]^T$ and dynamic obstacles, including other agents, move around the environment. In this scenario, the value of ρ is chosen as $\rho = 4$, prohibiting narrow passages.

The 3D trajectories followed by the UGVs and UAVs are presented in Fig. 4. The results demonstrate that the vehicles are able to successfully avoid collisions with obstacles and other agents, and safely reach the rendezvous location. To highlight this, Fig. 4 shows the evolution of the positions of a dynamic obstacle with $[x(t), y(t), z(t)]^T$ as it passes close to UAV 2 (in green) at $t = 16$ s, which successfully avoids it.

Similarly, Fig. 5 highlights the UGVs avoiding inter-agent collisions. The global paths generated by the A^* algorithm, along with the trajectories generated by the MPC controllers for the UGVs are presented in Fig. 5. Each UGV follows the global path smoothly while respecting its constraints, and successfully avoids collisions with other UGVs by switching to the virtual goal strategy then going back to the global path once it is safe.

When sufficiently close, each UAV starts its landing maneuver to land on its corresponding UGV. Therefore, the weight Q_z increases gradually according to the horizontal distance between the UGV and UAV as presented in Fig. 6, and the UAV finally lands at $z = 0.5$ m.

4.2 Scenario 2

In this second scenario, a different set of ground obstacles is tested. Initially the value of ρ is chosen as $\rho = 2$. As can be seen in Fig. 7, some passages between close obstacles are blocked and so the UGVs find safe routes around them while avoiding each other. On the other hand, when the value of ρ is increased to $\rho = 10$, the same passages are cleared. As demonstrated in Fig. 8, UGV 2 is then able to pass between the obstacles to reach its rendezvous point, highlighting the influence of the choice of ρ in generating less or more conservative paths.

Finally, the advantage of the obstacle aggregation strategy is demonstrated in Table 1, where the computation of the MPC controllers, normalized with respect to the no aggregation case, are presented. In both scenarios, the obstacle aggregation formulation has a reduced average computation time compared to that of the formulation with separate obstacle constraints. This highlights the

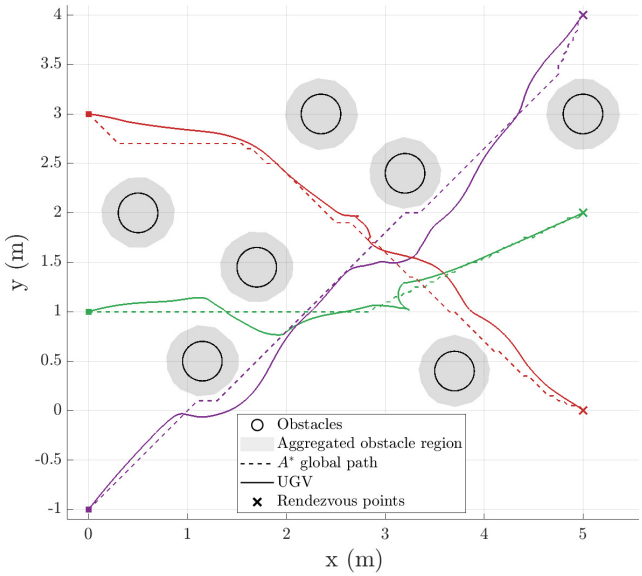


Fig. 8. Trajectories followed by UGV with $\rho = 10$.

Table 1. Metrics

Metric	Scenario	Vehicle	No agg.	Agg.
Normalized Comp. Time	1	UGV	1	1-0.32
		UAV	1	1-0.29
	2	UGV	1	1-0.34
		UAV	1	1-0.28
Path tracking RMSE (m)	1	UGV	0.089	0.073
	2	UGV	0.095	0.099

ability of this approach to improve the scalability of the system since as the number of obstacles and agents increases, the computation time increases significantly for the latter formulation. Moreover, the path tracking errors of the UGVs with respect to the A^* path are similar in both cases. Note that the values presented in the table correspond to the vehicle with the largest error.

5. CONCLUSION

In this work, a distributed MPC formulation for the rendezvous of multiple UAV-UGV pairs in a dynamic environment is presented. The safety of the agents is ensured through combining an obstacle aggregation and a recursive feasibility strategy in a cluttered environment. Simulation results demonstrate the effectiveness of the approach where multi-agents successfully rendezvous while avoiding static and dynamic obstacles as well as inter-agent collisions. Compared to a similar formulation that considers separate constraints for each obstacle, this approach exhibits improved computational efficiency.

Future work aims to extend the framework to minimize the mission time for the rendezvous problem and to account for obstacles of different shapes. The validation of the approach on higher fidelity models will also be further studied. Moreover, fallback strategies similar to Rubinacci et al. (2025) could be incorporated to deal with communication delays.

REFERENCES

Andersson, J.A.E., Gillis, J., Horn, G., Rawlings, J.B., and Diehl, M. (2019). CasADi – A software framework for nonlinear optimization and optimal control. *Mathematical Programming Computation*, 11(1), 1–36.

Asghar, A.B., Shi, G., Karapetyan, N., Humann, J., Reddinger, J.P., Dotterweich, J., and Tokekar, P. (2023). Risk-aware recharging rendezvous for a collaborative team of UAVs and UGVs. In *2023 IEEE International Conference on Robotics and Automation (ICRA)*, 5544–5550. London, United Kingdom.

Bacheti, V.P., Brandão, A.S., and Sarcinelli-Filho, M. (2021). A path-following controller for a UAV-UGV formation performing the final step of last-mile-delivery. *IEEE Access*, 9, 142218–142231.

Chai, R., Guo, Y., Zuo, Z., Chen, K., Shin, H.S., and Tsourdos, A. (2024). Cooperative motion planning and control for aerial-ground autonomous systems: Methods and applications. *Progress in Aerospace Sciences*, 146, 101005.

Daly, J.M., Ma, Y., and Waslander, S.L. (2015). Coordinated landing of a quadrotor on a skid-steered ground vehicle in the presence of time delays. *Autonomous Robots*, 38(2), 179–191.

Guo, J., Dong, X., Gao, Y., Li, D., and Tu, Z. (2022). Simultaneous obstacles avoidance and robust autonomous landing of a UAV on a moving vehicle. *Electronics*, 11(19), 3110.

Kozłowski, K. and Pazderski, D. (2004). Modeling and control of a 4-wheel skid-steering mobile robot. *International Journal of Applied Mathematics and Computer Science*, 14(4), 477–496.

Masry, G., Vieira, D., Orjuela, R., Meurer, T., and Basset, M. (2025). Cooperative aerial-ground vehicle rendezvous with integrated obstacle avoidance. In *2025 11th International Conference on Control, Decision and Information Technologies (CoDIT)*, 2202–2207. Split, Croatia.

Munasinghe, I., Perera, A., and Deo, R.C. (2024). A comprehensive review of UAV-UGV collaboration: advancements and challenges. *Journal of Sensor and Actuator Networks*, 13(6), 81.

Oh, D., Lim, Y., Jung, H., Huh, J., Lee, J., Choi, C., Kim, H.J., and Park, J. (2025). A survey on collision avoidance algorithms for multi-robot systems. *International Journal of Control, Automation and Systems*, 23(7), 2019–2035.

Rubinacci, R., Nazzari, A., and Lovera, M. (2025). Anytime trajectory optimization for multi-drone systems with guaranteed collision avoidance. *IEEE Control Systems Letters*, 9, 1255–1260.

Sankaranarayanan, V.N., Saradagi, A., Satpute, S., and Nikolakopoulos, G. (2024). Collision-Free Landing of Multiple UAVs on Moving Ground Vehicles Using Time-Varying Control Barrier Functions. In *2024 American Control Conference (ACC)*, 3760–3767. Toronto, ON, Canada.

Yu, S., Shen, C., Dallas, J., Epureanu, B.I., Jayakumar, P., and Ersal, T. (2025). A real-rime terrain-adaptive local trajectory planner for high-speed autonomous off-road navigation on deformable terrains. *IEEE Transactions on Intelligent Transportation Systems*, 26(3), 3324–3340.